Published in final edited form as:
Magn Reson Imaging. 2009 May ; 27(4): 570–576. doi:10.1016/j.mri.2008.08.008.

Respiratory motion-corrected proton magnetic resonance spectroscopy of the liver☆

Susan M. Noworolski[a,b,*], **Phyllis C. Tien**[c], **Raphael Merriman**[d], **Daniel B. Vigneron**[a,b], and **Aliya Qayyum**[a]

[a] Department of Radiology and Biomedical Imaging, University of California, San Francisco, San Francisco, CA

[b] The Graduate Group in Bioengineering, University of California, San Francisco and Berkeley, San Francisco and Berkeley, CA

[c] Department of Medicine, University of California, San Francisco and San Francisco Veteran Affairs Medical Center, San Francisco, CA

[d] Department of Gastroenterology, California Pacific Medical Center, San Francisco, CA

Abstract

Purpose—To develop a post-processing, respiratory-motion correction algorithm for magnetic resonance spectroscopy (MRS) of the liver and to determine the incidence and impact of respiratory motion in liver MRS.

Materials and Methods—One hundred thirty-two subjects (27 healthy, 31 with nonalcoholic fatty liver disease and 74 HIV-infected with or without hepatitis C) were scanned with free breathing MRS at 1.5 T. Two spectral time series were acquired on an 8-ml single voxel using TR/TE=2500 ms/30 ms and (1) water suppression, 128 acquisitions, and (2) no water suppression, 8 acquisitions. Individual spectra were phased and frequency aligned to correct for intrahepatic motion. Next, water peaks more than 50% different from the median water peak area were identified and removed, and remaining spectra averaged to correct for presumed extrahepatic motion. Total CH_2+CH_3 lipids to unsuppressed water ratios were compared before and after corrections.

Results—Intrahepatic-motion correction increased the signal to noise ratio (S/N) in all cases (median=11-fold). Presumed extrahepatic motion was present in 41% (54/132) of the subjects. Its correction altered the lipids/water magnitude (magnitude change: median=2.6%, maximum=290%, and was >5% in 25% of these subjects). The incidence and effect of respiratory motion on lipids/water magnitude were similar among the three groups.

☆This work was supported in part by grants R01 DK061738-SI, RO1 DK074718-01, K23-AI 66943 and P01 HD40543 from the NIH, as well as funding from the Society of Gastrointestinal Radiologists, the UCSFAcademic Senate, the GCRC Clinical Research Feasibility Fund Award and the UCSF Hellman Early Career Faculty Award. The Women's Interagency HIV Study (WIHS) is funded by the National Institute of Allergy and Infectious Diseases (UO1-AI-35004, UO1-AI-31834, UO1-AI-34994, UO1-AI-34989, UO1-AI-34993 and UO1-AI-42590) and by the National Institute of Child Health and Human Development (UO1-HD-32632). WIHS is co-funded by the National Cancer Institute, the National Institute on Drug Abuse and the National Institute on Deafness and Other Communication Disorders. Funding is also provided by the National Center for Research Resources (MO1-RR-00071, MO1-RR-00079, MO1-RR-00083).

*Corresponding author. Department of Radiology and Biomedical Imaging, The University of California, San Francisco, 185 Berry St, Suite 350, San Francisco, CA 94107, USA. Tel.: 415 353 9409; fax: 415 353 9423. sue@radiology.ucsf.edu (S.M. Noworolski).

Conclusion—Respiratory-motion correction of free breathing liver MRS greatly increased the S/N and, in a significant number of subjects, changed the lipids/water ratios, relevant for monitoring subjects.

Keywords

Spectroscopy; Liver; Steatosis; Nonalcoholic fatty liver disease; Respiration; Motion correction

1. Introduction

Hepatic steatosis (the presence of excessive fat within hepatocytes) is becoming increasingly prevalent [1]. Non-alcoholic fatty liver disease (NAFLD) is currently estimated to affect 20–30% of the US population and is integrally related to obesity and insulin resistance [1,2]. NAFLD is fundamentally defined by excessive hepatic steatosis in the absence of significant alcohol use and can progress from simple steatosis through steatohepatitis to cirrhosis and end-stage liver disease, even requiring liver transplantation. Steatosis has also been associated with viral infections. Both hepatitis C virus (HCV) infection and human immunodeficiency virus (HIV) infection have been associated with steatosis; HIV therapy has also been associated [3]. The prevalence of steatosis may be higher in HIV/HCV-coinfected than HCV-monoinfected patients [4]. Both steatosis and HCV can separately lead to further liver necroinflammation and fibrosis [5–7], which may confound the noninvasive assessment of steatosis.

Liver biopsy is the current gold standard to determine the severity of steatosis [8]. With the increased prevalence of steatosis and awareness of its implications in the development and progression of diverse liver diseases [1], there is increased need to noninvasively and precisely quantify hepatic steatosis. Diet, exercise and therapeutic interventions are being suggested to reduce the amount of lipids in the liver [9–11]. To properly monitor change in patients and the effectiveness of such interventions, an accurate, reliable, noninvasive measure of steatosis is required.

Magnetic resonance spectroscopy (MRS) has the potential to provide such a noninvasive assessment of steatosis. Ex vivo and animal studies have shown MRS to give an accurate measurement of liver fat [12–16]. In studies of fatty liver disease of diverse causes, MRS has demonstrated the ability to discriminate elevated hepatic lipids from normal [17–20]. However, the lack of any respiratory motion correction is a limitation of these studies, leading to relatively low signal to noise ratio (S/N), MRS spectra and the potential for less accuracy, possibly limiting the utility of this modality.

Acquisitions with greater S/N, and potentially with water suppression, are required to monitor small changes in hepatic fat, to analyze the effect of interventions and to have the potential to measure additional peaks beyond the dominant lipid peak [due to $(CH_2)n$]. Invariably, these acquisition requirements would lead to longer acquisition times and thus greater potential for motion artifacts. In earlier studies, the effect of respiratory motion on MRS measured lipids/water ratio has not been investigated. Respiratory motion may have differing effects in different disease populations. The high hepatic lipid content in patients with NAFLD and the common co-existence of inflammation and/or fibrosis in the HCV-infected patients may lead to greater variability in the measured MRS signals within the liver and between liver parenchyma and extrahepatic tissues (such as vessels) as compared to healthy controls.

Therefore, the aims of this study were (1) to develop a post-processing, respiratory motion-correction algorithm for liver MRS and (2) to determine the incidence and impact of

respiratory motion on free-breathing, liver MRS lipids/water measures in three groups: healthy controls, NAFLD patients and HIV-infected patients with or without HCV infection.

2. Materials and methods

2.1. Study subjects

MR imaging and spectroscopy were performed in 132 subjects: 27 healthy volunteers, 31 patients undergoing assessment of NAFLD and 74 HIV-infected patients, 44 of whom were coinfected with HCV. Demographics of the subjects are given in Table 1. Healthy volunteers had no evidence of fatty liver disease by in- and out-of-phase MR imaging and were free of HIV and HCV disease by report. The subjects with NAFLD all had histological confirmation of pathologic steatosis — greater than 5% of hepatocytes containing fat. The women with HIV and HCV coinfection were recruited from the Women's Interagency HIV Study [21,22]. Written informed consent was obtained from all subjects following a protocol approved by the Committee on Human Research at this institution.

2.2. MR Acquisition

The MR exam was performed on a 1.5-T GE clinical scanner using a torso phased array for signal reception. MR imaging included coronal and axial breath-held T_1-weighted images and fat suppressed, T_2-weighted, fast spin echo axial imaging (TE=100, echo train length=8, 8-mm-thick slices with 1-mm-thick gaps) used for MR spectroscopy (MRS) prescription. For MRS, an 8-ml voxel was placed in the liver, avoiding vessels and away from the edges of the liver in all dimensions (see Fig. 1 for a typical location). The MRS was acquired using a chemical shift selective, water-suppressed, 128 acquisition time series of point resolved spectroscopy single voxels (TR=2500 ms, TE=30 ms). Unsuppressed water spectra with eight acquisitions were also acquired at each location. An additional four spectra were acquired at the start of each acquisition, but not recorded, to ensure that an equilibrium state had been reached.

2.3. MR Processing

The respiratory motion-correction approach we used was to apply (1) an individual spectral frequency- and phase-correction scheme, similar to others [23–26], to reduce intrahepatic motion effects and (2) a novel artifact spectra identification and elimination correction scheme, similar in concept to Prescot et al. [27], for removal of signals from extrahepatic parenchyma, such as from hepatic vasculature.

First, each spectrum was individually Fourier transformed, and automatically phase and frequency shifted, based upon the water peak, using algorithms well established at our institution [28,29]. Even in the water-suppressed spectra, the residual water peak had sufficient S/N to allow this. Second, to evaluate extrahepatic motion, spectra were automatically assessed to identify spectra with water peaks more than 50% different from the median spectral peaks. A smaller cutoff value was avoided to ensure that small, biological variability would still be detected; the 50% cutoff detects shifts into markedly different tissues. Those abnormal spectra were eliminated and remaining artifact-free spectra were averaged. Peaks at 0.8, 1.2, 2.0, 2.2 and 5.3 ppm were integrated. These peaks represent CH_3 lipids (0.8 ppm), (CH_2)n lipids (1.2 ppm), other CH_2 lipids (2.0 and 2.2 ppm) and CH lipids (5.3 ppm). To calculate the total lipids, only the peaks attributed to CH_2 and CH_3 were summed, as the CH peak is complicated by overlap with water. The unsuppressed water spectra were similarly analyzed, and unsuppressed water peak areas at 4.7 ppm were calculated. Total lipids/water area ratios were calculated for each subject using the total lipids measure from the suppressed water sequence and the unsuppressed water measure from the unsuppressed water sequence.

The incidence of extrahepatic respiratory motion in the healthy volunteers, the NAFLD patients and the HIV-infected patients was recorded and compared using a *z*-test with both the Yates correction for continuity and a Bonferroni correction for multiple comparisons. Descriptive statistics were calculated for the improvement in S/N after the individual spectral correction (intrahepatic motion correction). The effect of the artifact-spectral correction (extrahepatic motion correction) was evaluated by calculating the magnitude percent difference in the lipids/water ratios obtained after (1) only individual-spectral correction and (2) both individual-spectral correction and artifact-spectral correction, with the difference normalized to the lipids/water ratio after both corrections, as given in the following equation:

$$\%\mathrm{Diff}_{\mathrm{L/W}} = \left| \frac{\mathrm{L/W}_{\mathrm{ind,art-corrected}} - \mathrm{L/W}_{\mathrm{ind-corrected}}}{\mathrm{L/W}_{\mathrm{ind,art-corrected}}} \right| \quad (1)$$

where $\%\mathrm{Diff}_{\mathrm{L/W}}$ is the percent difference in lipids/water ratios, $\mathrm{L/W}_{\mathrm{ind,art\text{-}corrected}}$ is the lipids/water ratio after both individual-spectral corrections and artifact-spectral corrections, and $\mathrm{L/W}_{\mathrm{ind\text{-}corrected}}$ is the lipids/water ratio after individual-spectral corrections only.

Descriptive statistics were calculated, and the Kruskal–Wallis test was used to compare the distribution of values among the three groups. The JMP statistical software package was used for statistical analyses (SAS Institute, Cary, NC, USA).

3. Results

Fig. 1 shows example images of the spectral location and the resultant spectra. The acquisition of a time series of spectra allowed the evaluation of respiratory or other temporal variations. In all cases, the phase varied greatly among individual spectra, with some spectra 180° out of phase with other spectra. Correcting for such phase differences greatly increased the S/N of the resultant summed spectrum. In an example case, shown in Fig. 2, the S/N of the CH_2 lipid peak (as compared to the noise in the spectrum) was measured as 17:1 when not corrected, but increased to 238:1 when corrected for individual spectral variations, a 14-fold difference. The S/N increased in all cases, with a median of 11-fold improvement and a range from 1.3-fold to 159-fold improvement.

A substantial number of subjects (41%, 53/132) had water peak areas that varied more than 50% from the median values (indicating probable extrahepatic motion effects). The incidence of water peak areas that varied more than 50% from the median values was not significantly different among the three groups (13/27 healthy subjects, 14/31 with NAFLD and 26/74 with HIV+). This motion artifact occurred in 4.4% (797/17,952) of the spectra acquired. Fig. 3 presents an example of three consecutive spectra that show a large change in water amplitude. Subjects with this presumed extrahepatic motion yielded a median of 2.6% in the magnitude percent difference of lipids/water ratios obtained after (1) only individual-spectral correction and (2) both individual-spectral correction and artifact-spectral correction, with differences normalized to the lipids/water ratio after both corrections [$\%\mathrm{Diff}_{\mathrm{L/W}}$, see Eq. (1)]. These magnitude percentage differences in lipids/water ratios are plotted in Fig. 4 and were not significantly different among the three populations ($P<.64$, Kruskal–Wallis test). The majority of these subjects (78%) had the lipids/water ratios higher after both motion corrections than after the individual spectra only corrected measures. In 11% (14/132) of the subjects, the $\%\mathrm{Diff}_{\mathrm{L/W}}$ was greater than 5%. Differences ranged as high as 290%. In this extreme case, the lipids/water ratio was 0.27 after only individual-spectral corrections, but decreased to 0.07 after further correction.

4. Discussion

Respiratory motion-associated movement of the liver can potentially cause MR data to originate from different locations within liver parenchyma, a vessel or even outside the liver. A study of abdominal motion showed the diaphragm typically moved 15–20 mm during free breathing [30]. Even with a metabolic liver disease like NAFLD in which steatosis has been shown histologically to be diffusely and equally distributed [31], respiration will affect the MR spectra, causing phase shifts [32]. In liver spectroscopy studies, typically a number of spectra are acquired and automatically averaged, with only the final averaged spectrum saved. Without taking into account respiratory motion, the final averaged spectrum may be inaccurate.

Performing individual-spectral correction before averaging the acquired spectra significantly increased the S/N in the liver spectra in this study. The individual spectral phase variations in the spectra were likely due to intrahepatic motion (as opposed to extrahepatic motion) during the spectral acquisition. This approach to dealing with the phase shifts caused by respiratory motion was proposed by Zhu et al. [23] and further shown by others [24,25], though this correction was only demonstrated in a limited number of subjects. Additionally, only one of these studies acquired spectra in the liver, in which the single subject was a healthy volunteer [24]. However, this technique of phasing individual spectra before combining them has also been applied in the brain to correct for smaller motion [26].

This correction cannot eliminate artifacts beyond frequency and phase variations, such as might result from shifts into different tissues. The approach in this study to deal with such extrahepatic motion was to identify spectra with large changes in the water peak area (50% different from the median) and then remove them before averaging the spectra. The same approach can and has been applied to identify such changes in the fat peak area rather than or in addition to changes in the water peak area. Prescot et al. [27] also applied a similar technique to eliminate individual spectra from a time series of single voxel spectra obtained from the gallbladder. They used the presence of a large $(CH_2)n$ lipid peak at 1.2 ppm, based upon in vitro studies, as their criteria for elimination [27]. In the current study, 41% of subjects had large changes in their lipids/water ratio during the spectral acquisition, likely due to motion-induced shifting from hepatic to extrahepatic tissue, indicating that such motion is common in liver MRS and that neighboring tissue can have very different water MRS signals. This motion caused, in general, a 2.6% change in the resultant lipids/water ratios. Such a change may not be very significant when simply identifying fat in the liver; however, it can be variable and may be significant when assessing subtle changes in hepatic steatosis that might result from therapeutic intervention. In 11% of subjects, such respiratory motion caused greater than 5% change in the lipids/water ratio, with differences ranging as high in magnitude as 290%. In this extreme case, the lipids/water ratio was 0.27 after only individual phase corrections, suggestive of Grade 2 or 3 steatosis [19] (steatosis grading relies on the percentage of hepatocytes containing fat: Grade 0: <5%, Grade 1: 5–33%, Grade 2: 33–66%, Grade 3: >66% [8]). In contrast, the corrected lipids/water ratio (0.07) indicated a low Grade 1 steatosis [19]. Such artifactual variation could cause significant misinterpretation of the liver MRS result, particularly if assessing the effects of an intervention. Additionally, as the size of this artifactual effect on the lipids/water ratio is variable, study design sample size calculations could be impacted significantly if this correction was not applied.

Other potential approaches to dealing with respiratory motion in liver MRS include breath-holding and respiratory gating. Breath-held liver MRS has been attempted and did reduce the variability of measurements [32], but cannot provide the higher S/N of longer sequences. Respiratory gating, often used in MR, would be expected to reduce motion artifacts,

particularly of small amounts of motion. However, variable intensity of breathing could lead to different tissues being sampled at the same phase of the respiratory cycle. Such large motion artifact would not be corrected with respiratory gating. Also, respiratory gating would lead to individual scans being acquired at differing intervals, leading to data that would be dependent upon the tissue MR relaxation times, the acquisition scan times, the subjects' breathing patterns and the actual MRS compound concentrations, which would greatly confound interpretation of the MRS data. As additional spectra with respiratory gating were not acquired in this study, a direct comparison of the two techniques is not possible as part of this study.

While large respiratory motion from spectrum to spectrum was corrected in this study, any motion within the acquisition of a single spectrum was not corrected. As the time between excitation and measurement was only 30 ms, such motion was assumed to be small and not of significance. While respiratory motion caused a median magnitude difference in the lipids/water ratio of 2.6%, this was due in part to the long time series of spectra acquired (128), such that artifacts in just a few spectra would not have a large impact on the final average. However, shorter acquisitions would be much more susceptible to motion effects. One such example is the unsuppressed water acquisition performed in this study, with only eight acquisitions. In one case, one of these eight spectra had virtually no signal, leading to a 12.5% difference in the water signal measured. When artifacts did occur in the spectra, the lipids/water ratios in those artifactual spectra were generally quite different from the remainder, so final averaged ratios would also be different if the artifactual spectra were included and lipids/water ratios from the same acquisition were calculated.

A limitation of this technique was that the large changes in the water peak area during the measurement were presumed to be due to extrahepatic motion and corresponding spectra were eliminated. This would not be suitable if dynamic biological changes were expected in the tissue of interest. Additionally, this correction retains spectra with similar water peak areas and reports them as the desired spectra. In actuality, the presented extrahepatic motion-correction scheme yields spectra from the most commonly sampled tissue, which may not be the desired location. As the current study is not investigating a dynamic process during the acquisition and as only 4.4% of the spectra in this study had extrahepatic motion, this limitation is not expected to be a concern in this study.

Our assessment and correction of respiratory motion indicate that the presented, longer, free breathing, water suppressed acquisition can be used to evaluate the liver lipids/water ratios free of respiratory motion artifacts. Also, this acquisition has the potential to provide increased sensitivity due to higher S/N and increased characterization due to increased spectral information, which may be useful for measuring subtle changes in steatosis and for assessing liver disorders beyond steatosis.

This technique was fully automatic and, as such, could be implemented on scanners. However, the algorithm was based upon characteristics of the spectra studied. First, individual spectra were required to be stored and were required to have sufficient water S/N to allow individual phasing. In low S/N applications, a modified water suppression scheme could be utilized to retain sufficient water S/N. Second, the spectral peaks were expected to have the same phasing as the water peak. Third, the water peak region was known and used in the automatic frequency- and phase-correction routine. Additionally, as mentioned above, the motion was expected to be a small fraction of the acquisition, such that the final averaged spectrum represented a tissue type most frequently sampled and not necessarily the desired tissue. Automatic implementation of this algorithm for applications beyond the one presented would require assessment and confirmation of these criteria or could lead to misinterpretation of the resultant spectra.

In conclusion, this study showed that individual spectral frequency- and phase correction of liver MRS increased the S/N's for all subjects. It is recommended that this be standard practice for all MRS studies susceptible to respiratory or other similar motion artifact. Extrahepatic motion (such as into a vessel) occurred frequently and in some cases caused significant change in the lipids/water ratios with the potential to adversely impact the accurate interpretation of the liver MRS results. Therefore, to obtain a sensitive, high S/N MRS measure of hepatic steatosis, we advocate both intrahepatic and extrahepatic respiratory motion correction of a time series of MRS data. This may be particularly important with increasing MRS use to evaluate the effects of diet, exercise and other therapeutic interventions in ameliorating hepatic steatosis.

References

1. Neuschwander-Tetri BA, Caldwell SH. Nonalcoholic steatohepatitis: summary of an AASLD Single Topic Conference. Hepatology 2003;37 (5):1202–19. [PubMed: 12717402]
2. Scheen AJ, Luyckx FH. Obesity and liver disease. Best Pract Res Clin Endocrinol Metab 2002;16(4):703–16. [PubMed: 12468416]
3. Hadigan C, Liebau J, Andersen R, Holalkere NS, Sahani DV. Magnetic resonance spectroscopy of hepatic lipid content and associated risk factors in HIV infection. J Acquir Immune Defic Syndr 2007;46(3):312–7. [PubMed: 17721396]
4. Gaslightwala I, Bini EJ. Impact of human immunodeficiency virus infection on the prevalence and severity of steatosis in patients with chronic hepatitis C virus infection. J Hepatol 2006;44(6):1026–32. [PubMed: 16618518]
5. McCullough AJ. The clinical features, diagnosis and natural history of nonalcoholic fatty liver disease. Clin Liver Dis 2004;8 (3):521–33. viii. [PubMed: 15331061]
6. Poynard T, Bedossa P, Opolon P. Natural history of liver fibrosis progression in patients with chronic hepatitis C. The OBSVIRC, METAVIR, CLINIVIR, and DOSVIRC groups. Lancet 1997;349 (9055):825–32. [PubMed: 9121257]
7. Clouston AD, Jonsson JR, Powell EE. Steatosis as a cofactor in other liver diseases: hepatitis C virus, alcohol, hemochromatosis, and others. Clin Liver Dis 2007;11(1):173–89. [PubMed: 17544978]
8. Kleiner DE, Brunt EM, Van Natta M, Behling C, Contos MJ, Cummings OW, et al. Design and validation of a histological scoring system for nonalcoholic fatty liver disease. Hepatology 2005;41(6):1313–21. [PubMed: 15915461]
9. Huang MA, Greenson JK, Chao C, et al. One-year intense nutritional counseling results in histological improvement in patients with non-alcoholic steatohepatitis: a pilot study. Am J Gastroenterol 2005;100 (5):1072–81. [PubMed: 15842581]
10. Neuschwander-Tetri BA, Brunt EM, Wehmeier KR, Oliver D, Bacon BR. Improved nonalcoholic steatohepatitis after 48 weeks of treatment with the PPAR-gamma ligand rosiglitazone. Hepatology 2003;38(4):1008–17. [PubMed: 14512888]
11. Federico A, Niosi M, Vecchio Blanco CD, Loguercio C. Emerging drugs for non-alcoholic fatty liver disease. Expert Opin Emerg Drugs 2008;13(1):145–58. [PubMed: 18321154]
12. Rosen BR, Carter EA, Pykett IL, Buchbinder BR, Brady TJ. Proton chemical shift imaging: an evaluation of its clinical potential using an in vivo fatty liver model. Radiology 1985;154:469–72. [PubMed: 3966134]
13. Bollard ME, Garrod S, Holmes E, et al. High-resolution (1)H and (1)H-(13)C magic angle spinning NMR spectroscopy of rat liver. Magn Reson Med 2000;44(2):201–7. [PubMed: 10918318]
14. Foley LM, Towner RA, Painter DM. In vivo image-guided (1)H-magnetic resonance spectroscopy of the serial development of hepatocarcinogenesis in an experimental animal model. Biochim Biophys Acta 2001;1526(3):230–6. [PubMed: 11410331]
15. Thomsen C, Becker U, Winkler K, Christoffersen P, Jensen M, Henriksen O. Quantification of liver fat using magnetic resonance spectroscopy. Magn Reson Imaging 1994;12(3):487–95. [PubMed: 8007779]

16. Longo R, Pollesello P, Ricci C, et al. Proton MR spectroscopy in quantitative in vivo determination of fat content in human liver steatosis. J Magn Reson Imaging 1995;5(3):281–5. [PubMed: 7633104]

17. Szczepaniak LS, Babcock EE, Schick F, Dobbins RL, Garg A, Burns DK, et al. Measurement of intracellular triglyceride stores by H spectroscopy: validation in vivo. Am J Physiol 1999;276(5 Pt 1):E977–89. [PubMed: 10329993]

18. Longo R, Ricci C, Masutti F, Vidimari R, Croce LS, Bercich L, et al. Fatty infiltration of the liver: quantification by ^{1}H localized magnetic resonance spectroscopy and comparison with computed tomography. Invest Radiol 1993;28(4):297–302. [PubMed: 8478169]

19. Noworolski SM, Tien P, Westphalen A, Merriman R, Vigneron DB, Qayyum A. MR Spectroscopy of non-alcoholic fatty liver disease. Proc Int Soc Magn Reson Med 2005:11 . abstract 336.

20. Thomas EL, Hamilton G, Patel N, O'Dwyer R, Dore CJ, Goldin RD, et al. Hepatic triglyceride content and its relation to body adiposity: a magnetic resonance imaging and proton magnetic resonance spectroscopy study. Gut 2005;54(1):122–7. [PubMed: 15591516]

21. Barkan SE, Melnick SL, Preston-Martin S, et al. The Women's Interagency HIV Study. Epidemiology 1998;9:117–25. [PubMed: 9504278]

22. Bacon MC, von Wyl V, Alden C, et al. The Women's Interagency HIV Study: an observational cohort brings clinical sciences to the bench. Clin Diagn Lab Immunol 2005;12:1013–9. [PubMed: 16148165]

23. Zhu G, Gheorghiu D, Allen PS. Motional degradation of metabolite signal strengths when using STEAM: a correction method. NMR Biomed 1992;5(4):209–11. [PubMed: 1449957]

24. Star-Lack JM, Adalsteinsson E, Gold GE, Ikeda DM, Spielman DM. Motion correction and lipid suppression for ^{1}H magnetic resonance spectroscopy. Magn Reson Med 2000;43(3):325–30. [PubMed: 10725872]

25. Gabr RE, Sathyanarayana S, Schar M, Weiss RG, Bottomley PA. On restoring motion-induced signal loss in single-voxel magnetic resonance spectra. Magn Reson Med 2006;56(4):754–60. [PubMed: 16964612]

26. Helms G, Piringer A. Restoration of motion-related signal loss and line-shape deterioration of proton MR spectra using the residual water as intrinsic reference. Magn Reson Med 2001;46(2): 395–400. [PubMed: 11477645]

27. Prescot AP, Collins DJ, Leach MO, Dzik-Jurasz AS. Human gallbladder bile: noninvasive investigation in vivo with single-voxel ^{1}H MR spectroscopy. Radiology 2003;229(2):587–92. [PubMed: 14526094]

28. Nelson S, Brown T. A new method for automatic quantification of 1-D spectra with low signal to noise ratio. J Magn Reson Imaging 1987;84:95–109.

29. Nelson SJ. Analysis of volume MRI and MR spectroscopic imaging data for the evaluation of patients with brain tumors. Magn Reson Med 2001;46(2):228–39. [PubMed: 11477625]

30. Schwarz A, Leach M. Implications of respiratory motion for the quantification of 2D MR spectroscopic imaging data in the abdomen. Phys Med Biol 2000;45(8):2105–16. [PubMed: 10958183]

31. Merriman RB, Ferrell LD, Patti MG, Weston SR, Pabst MS, Aouizerat BE, et al. Correlation of paired liver biopsies in morbidly obese patients with suspected nonalcoholic fatty liver disease. Hepatology 2006;44(4):874–80. [PubMed: 17006934]

32. Katz-Brull R, Rofsky NM, Lenkinski RE. Breathhold abdominal and thoracic proton MR spectroscopy at 3T. Magn Reson Med 2003;50(3):461–7. [PubMed: 12939752]

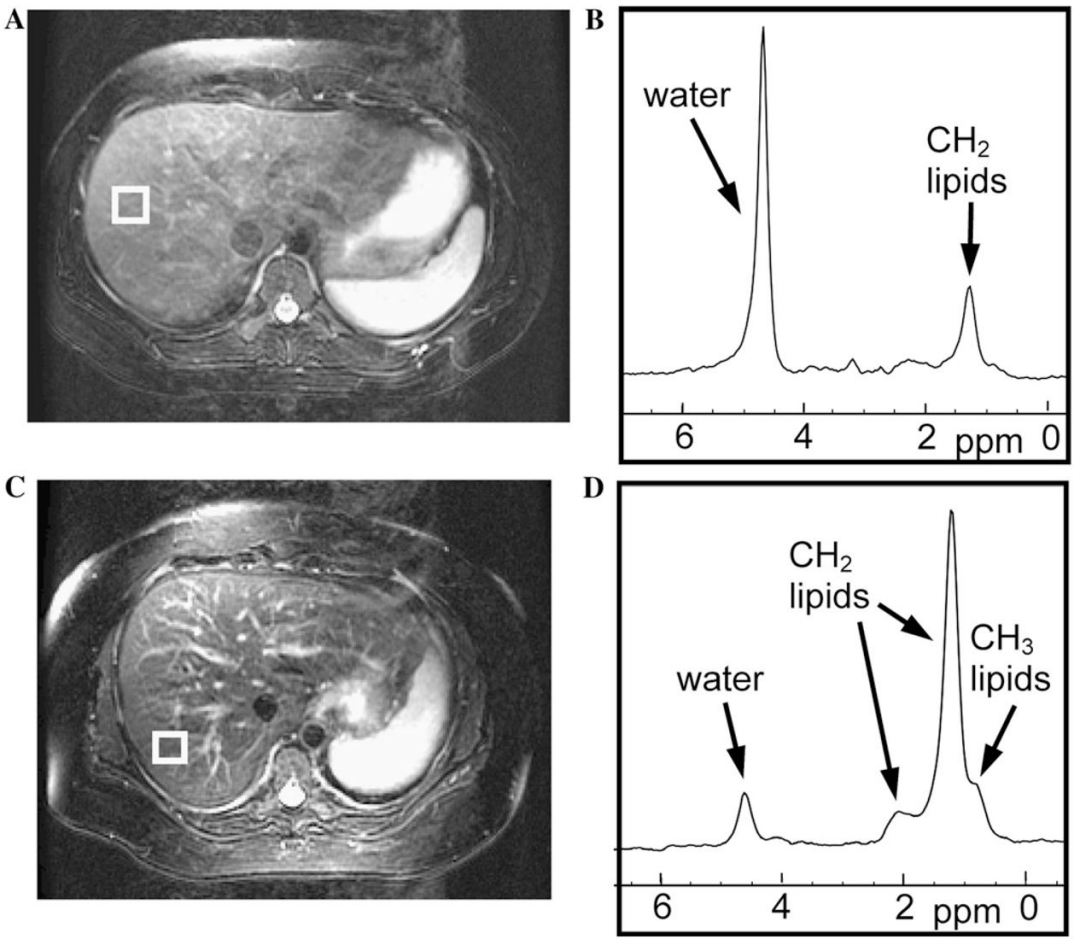

Fig. 1.

Example MR images and MR spectra. The top row example (A and B) is from a 22-year-old healthy female. The bottom row example (C and D) is from a 51-year-old female with NAFLD and Grade 2 steatosis. (A and C) T_2-weighted axial images showing the location of the MRS single voxel (white box). (B and D) Averaged, motion-corrected spectra showing water and lipid peaks.

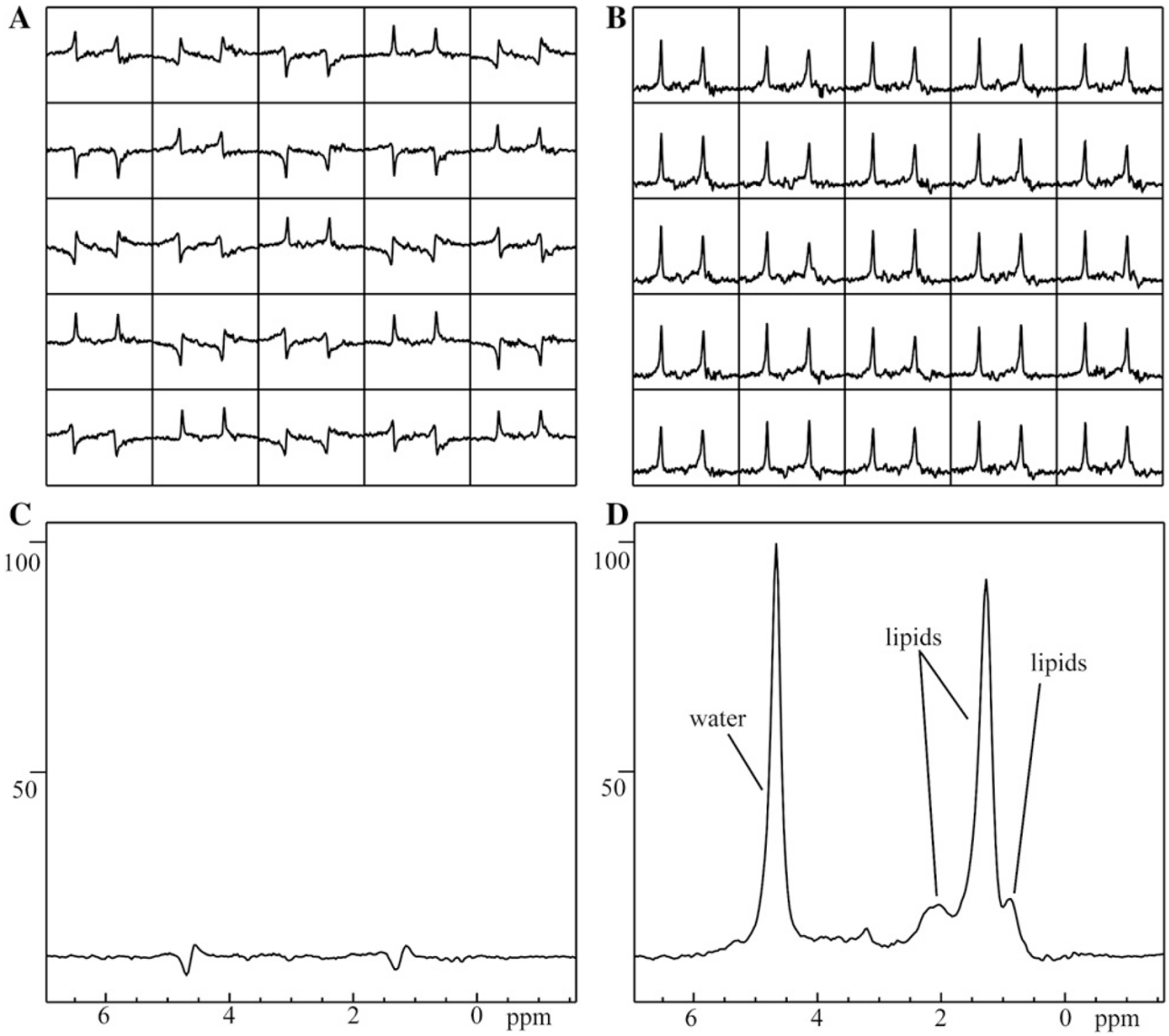

Fig. 2.

Respiration-induced phase differences reduce the S/N of the total lipids in the averaged spectrum from 238:1 to 17:1, a 14-fold difference. (A) Sample of spectra as acquired. (B) Sample of spectra from (A), frequency- and phase corrected. (C) Full set of 128 acquired spectra averaged without respiratory corrections performed and (D) corrected spectra averaged, shown on the same arbitrary scale as (C).

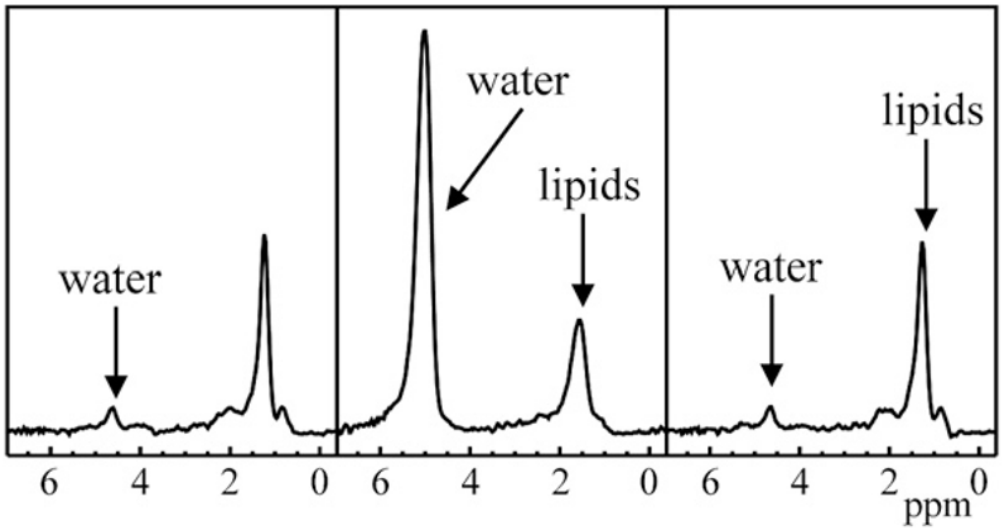

Fig. 3.
Three consecutive spectra from a subject showing large respiration or other artifact, presumed to be due to motion causing spectral acquisition from extrahepatic tissue.

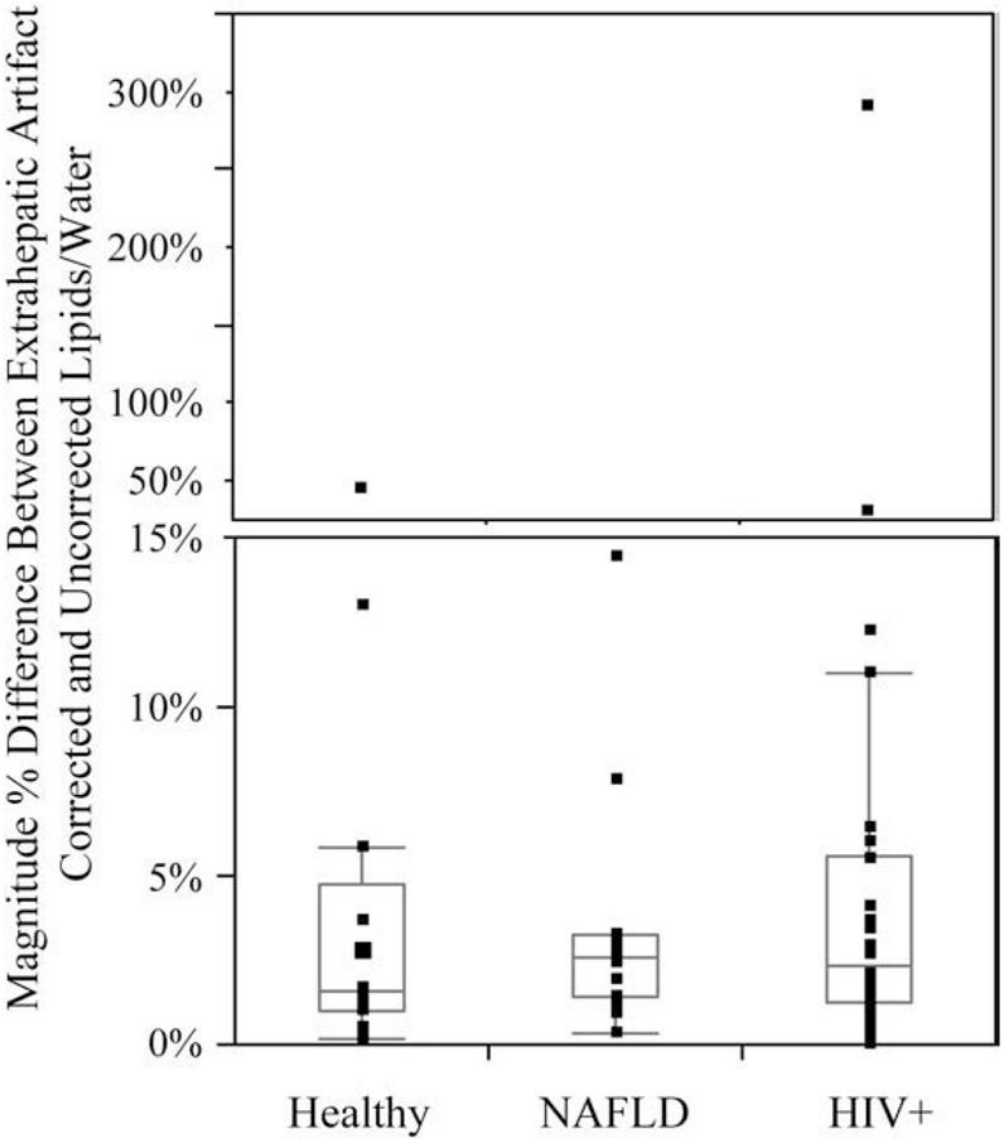

Fig. 4.

Box plot of magnitude % difference in lipids/water due to presumed extrahepatic respiratory motion ($\%\mathrm{Diff}_{L/W} = \left|\frac{L/W_{ind,art-corrected} - L/W_{ind-corrected}}{L/W_{ind,art-corrected}}\right|$, see the text for more details) for the three populations. The box indicates the first to third quartile values. The horizontal line within the box indicates the median and the whiskers (vertical lines) indicate the outermost data point that falls within the outer quartile+1.5×interquartile range. Individual points are indicated as dots. Note the upper portion has different scaling to plot the very large values.

Table 1

Subject demographics

	Healthy controls	NAFLD	HIV+
Number of subjects	27	31	74
Sex: male/female	5/22	14/17	23/51
Age (years)	37±11	45±14	47±7
BMI (kg/m^2)	27±7	30±6	26±6

Age and BMI are presented as mean±S.D